

Response to Reviewers comments – report #3

Dear Editor,

Following please find our point-by-point response to the two Referees' comments. Their comments are in regular font and our responses are in bold. The page and line numbers refer to the revised manuscript that will be submitted with this response (with "all mark up" display for review).

Referee #3, Report #2

This is my second review of this manuscript. While I think it has improved considerably with respect to the previous version, in particular in the description and treatment of the Budyko-parameter, I remain somewhat skeptical about the generality of the results. I generally like scaling analysis, but I think one should always make a clear distinction between an analysis that is supposed to represent the real-world, or a hypothetical ("first-order"/potential/etc) analysis that shows the potential effect under certain restrictive assumptions (such as the use of a constant Budyko parameter in this case). The authors do acknowledge the limitations of their approach, but I feel this could (and should) be better reflected in the text. In my view, the manuscript would read much better if "heterogeneity bias" is replaced everywhere by "potential/theoretical/hypothetical heterogeneity bias" (or similar), so the suggestion of it being an analysis of the complete system including (varying) land surface properties is removed. I leave it up to the authors to make the relatively minor textual changes needed to accommodate this final comment.

The term "heterogeneity bias" occurs 79 times in the text, and we do not think that adding "potential", "theoretical", or "hypothetical" 79 times would be an improvement. Where appropriate, we already refer to "estimated heterogeneity bias", "realistic estimates of the heterogeneity bias", "numerical estimates of the heterogeneity bias", "heterogeneity bias estimates", "heterogeneity bias in ET estimates", "heterogeneity bias in a hypothetical two-column model", and so forth. We also make clear that our goal is to identify spatial patterns in the heterogeneity bias, not its absolute magnitude.

We have reviewed all 79 occurrences of the phrase "heterogeneity bias", looking for any cases where it is not already clear from context that we are referring to a hypothetical calculation (or, alternatively, the general concept of heterogeneity bias, for which "hypothetical" would not apply anyhow). In the 12 cases where we could imagine that this was not already completely clear, we modified the text accordingly.

Referee #1, Report#3

I highlight below few more points where, in my opinion, authors response is still not fully convincing. I think that an additional effort to improve the manuscript along these points could eventually make the work suitable for publication in HESS.

- In the first and second review iteration I made clear about the weak link between this work and ESMs. A pragmatic way of avoiding any misunderstanding on this point is to start the abstract (lines 22-25 of the track-changes version of the manuscript) and the first paragraph of the introduction (lines 41-48) in a different way. In any case, I would remove any link to ESMs that could potentially mislead the reader.

We have removed any mention of ESM's from the abstract and have removed the first paragraph of the introduction almost entirely, line 42-49, (transferring only half a sentence into the second paragraph of the old introduction, which is now the first paragraph of the new introduction). These introductory statements now focus on "estimates of evapotranspiration" rather than ESM's.

- I suggested extending the analysis of the heterogeneity bias by clustering the results over different climate zones over the globe. I think this analysis is still useful even if using one single dataset for P (i.e., WCLim) and two datasets for PET (i.e., WCLim and MODIS). This effort could lead to additional discussion that eventually elevate the scientific significance of the work.

We appreciate the reviewer's perspective, but our own assessment of the usefulness of a global analysis is different. The advantages of confining this part of our analysis to the US are clear: we can compare the two precipitation data products (Prism and WorldClim) instead of having only one, and the observational constraints on both the P and PET data products are better in the US than over most of the globe. While we could of course ALSO do this analysis at global scale (but without Prism), we would prefer not to make the paper longer and more complicated at this stage.

- I appreciate authors effort in providing additional insights on the implications of using different n values. However, I would expect some more explanations on the physical mechanisms leading to larger biases by higher n values. Finally, I do not think that repeating the analysis with spatially-distributed n values could create "artifacts". This additional analysis will show the interplay between scale-dependency in P, PET, and n with respect to the heterogeneity bias in ET. Again, this could be an effective way of bringing the scientific aspects of the work on the front.

We now explain the effects of "n" as follows: "as expected from Eqs. 3 and 4, higher values of n lead to larger heterogeneity biases, because higher values of n localize the curvature of the Budyko function more strongly at the transition between the energy and water limits (Fig. 1b), increasing the heterogeneity bias for P/PET values near this transition." (Lines 393-400)

The problem with doing an analysis with spatially distributed n is this: how, and on what basis, should we assume that n varies from place to place? " n " is an empirical parameter, typically estimated by comparing mass balances from many catchments. Thus, it is an ensemble estimate over a group of catchments, and we do not have a solid basis for attributing different n values to individual catchments, let alone individual points on the landscape within catchments. Given that we have little or no information on how, and how much, n actually varies across real-world landscapes, we would prefer not to perform analyses based on arbitrary assumptions about spatial variability in n .

1 **Global assessment of how averaging over spatial heterogeneity in precipitation and potential evapotranspiration**
2 **affects modeled evapotranspiration rates**

3

4 Elham Rouholahnejad Freund^{1,2}, Ying Fan³, James W. Kirchner^{2,4,5}

5

6 ¹Laboratory of Hydrology and Water Management, Ghent University, Ghent, Belgium

7 ²Department of Environmental Systems Science, ETH Zurich, 8092, Zurich, Switzerland

8 ³Department of Earth and Planetary Sciences, Rutgers University, New Brunswick, NJ, United States

9 ⁴Swiss Federal Research Institute WSL, Birmensdorf, 8903, Switzerland

10 ⁵Dept. of Earth and Planetary Science, University of California, Berkeley, CA 94720, United States

11

12 *Correspondence to:* Elham Rouholahnejad Freund, elham.rouholahnejad@gmail.com

13

14 **Short summary**

15 Evapotranspiration (ET) rates and the properties that regulate them are spatially heterogeneous. Averaging over
16 spatial heterogeneity in precipitation and potential evapotranspiration as main drivers of ET may lead to biased
17 estimates of energy and water fluxes from the land surface to the atmosphere. Here we show that this bias will be
18 largest in mountainous terrain, in regions with temperate climates and dry summers, and in landscapes where
19 spatial variations in precipitation and potential evapotranspiration are inversely correlated.

20

21 **Abstract**

22 ~~Accurately estimating large-scale evapotranspiration rates is essential to understanding and predicting. The major~~
23 ~~goal of large-scale Earth System Models (ESMs) is to understand and predict~~ global change. Evapotranspiration
24 ~~models that are applied at continental scale typically. However, computational constraints require ESMs to~~ operate
25 on relatively large spatial grids ~~(typically ~1 degree or ~100 km in size)~~, with the result that the heterogeneity in
26 land surface properties and processes at smaller spatial scales cannot be explicitly represented. Averaging over this
27 spatial heterogeneity may lead to biased estimates of energy and water fluxes. Here we estimate how averaging
28 over spatial heterogeneity in precipitation (P) and potential evapotranspiration (PET) may affect grid-cell-averaged
29 evapotranspiration (ET) rates, as seen from the atmosphere over heterogeneous landscapes across the globe. Our
30 goal is to identify where, under what conditions, and at what scales this "heterogeneity bias" could be most
31 important, but not to quantify its absolute magnitude. We use Budyko curves as simple functions that relate ET to
32 precipitation (P) and potential evapotranspiration (PET). Because the relationships driving ET are nonlinear,
33 averaging over sub-grid heterogeneity in P and PET will lead to biased estimates of average ET. We examine the
34 global distribution of this bias, its scale dependence, and its sensitivity to variations in P versus PET. Our analysis
35 shows that this "heterogeneity bias" is more pronounced in mountainous terrain, in landscapes where spatial
36 variations in P and PET are inversely correlated, and in regions with temperate climates and dry summers. We also
37 show that this heterogeneity bias increases on average, and expands over larger areas, as the grid cell size
38 increases.

39
40

41 **1. Introduction**

42 Earth System Models (ESMs) are designed to understand interactions between the land surface, atmosphere, and
43 oceans and to predict global environmental changes. However, the Earth system and its underlying physical
44 processes are highly heterogeneous across orders of magnitude in scale below the scale of typical ESM grids (e.g.,
45 1° by 1°). Despite increasing recognition of the need to mechanistically represent physical processes in ESMs,
46 currently even the most disaggregated large scale ESMs cannot explicitly represent the spatial heterogeneity of
47 land surface hydrological properties at scales that are important to atmospheric fluxes. Averaging over land surface
48 properties at the scale of ESM model grid cells may have important implications for water and energy flux estimates
49 (Avisar and Pielke, 1989; Giorgi and Avissar, 1997; Ershadi et al., 2013; Lu et al., 2014).

50
51 Estimates of evapotranspiration (ET) fluxes have significant implications for future temperature predictions. Smaller
52 ET fluxes imply greater sensible heat fluxes and, therefore, drier and warmer conditions in the context of climate
53 change (Seneviratne et al., 2010). Surface evaporative fluxes (and thus energy partitioning over land surfaces) are
54 nonlinear functions of available water and energy, and thus are coupled to spatially heterogeneous surface
55 characteristics (e.g., soil type, vegetation, topography) and meteorological inputs (e.g., radiative flux, wind, and
56 precipitation; Kalma et al., 2008; Sharaeeni and Or, 2010; Holland et al., 2013). These characteristics are spatially
57 variable on length scales of <1 m to many kilometers. Even the highest-resolution continental-scale
58 evapotranspiration models, such as those that are embedded in Earth System Models (ESMs), typically cannot
59 explicitly represent the spatial heterogeneity of land surface hydrological properties at scales that are important to
60 atmospheric fluxes. Instead, these models usually, well below typical ESM grid scales of ~100 km, ESMs calculate
61 grid-averaged surface and atmospheric evapotranspiration fluxes based on using parameterizations that correspond
62 to grid-averaged properties of the land surface (Sato et al., 1989; Koster et al., 2006; Santanello and Peters-Lidard,
63 2011). Thus, ET estimates that are derived from spatially-averaged land surface properties do not capture ET
64 variations driven by the underlying surface heterogeneity (McCabe and Wood, 2006). These spatially averaged ET
65 estimates may differ from the average of the actual spatially heterogeneous ET flux, because the relationships
66 driving ET are nonlinear. Because the relationships driving ET are nonlinear, the average ET flux from a
67 heterogeneous landscape may be different from an ET estimate calculated from spatially averaged inputs
68 (Rouholahnejad Freund and Kirchner, 2017).

69
70 Several studies have quantified the effects of land surface heterogeneity on potential evapotranspiration (PET) and
71 latent heat (LH) fluxes, and have found that averaging over land surface heterogeneity can potentially bias ET
72 estimates either positively or negatively. For example, Boone and Wetzel (1998) studied the effects of soil texture
73 variability within each pixel in the Land-Atmosphere-Cloud Exchange (PLACE) model, which has a spatial resolution
74 of approximately 100 by 100 km. They reported that accounting for sub-grid variability in soil texture reduced
75 global ET by 17%, increased total runoff by 48%, and increased soil wetness by 19%, compared to using a
76 homogenous soil texture to describe the entire grid cell. Kollet (2009) found that heterogeneity in soil hydraulic

77 conductivity had a strong influence on evapotranspiration during the dry months of the year, but not during
78 months with sufficient moisture availability. Hong et al. (2009) reported that aggregating radiance data from 30 m
79 to 60, 120, 250, 500, and 1000 m resolution (input upscaling) and then calculating ET from these aggregated inputs
80 at these grid scales using Surface Energy Balance Algorithm for Land (SEBAL, Bastiaanssen et al., 1998a) yields
81 slightly larger ET estimates as compared to ET calculated with finer resolution inputs and then aggregated at the
82 desired grid scales (output upscaling). The discrepancy between ET estimated with the output upscaling method
83 and the input upscaling method grows as the size of the grid cell increases (the difference between ET calculated
84 from the input and output upscaling methods is ~20% more at a grid scale of 1 km by 1 km compared to a grid scale
85 of 120 m by 120 m). Aminzadeh et al. (2017) investigated the effects of averaging surface heterogeneity and soil
86 moisture availability on potential evaporation from a heterogeneous land surface including bare soil and vegetation
87 patches. They found that if the heterogeneity length scale is smaller than the convective atmospheric boundary
88 layer (ABL) thickness, averaging over heterogeneous land surfaces has only a small effect on average potential
89 evaporation rates. Averaging over larger-scale heterogeneities, however, led to overestimates of potential
90 evaporation.

91
92 Heterogeneity biases have also been identified in ET calculation algorithms that use remote sensing data as inputs.
93 McCabe and Wood (2006) found that remote sensing retrievals of ET are larger than the corresponding in-situ flux
94 estimates and characterized the roles of land surface heterogeneity and remote sensing resolution in the retrieval
95 of evaporative flux. McCabe and Wood (2006) used Landsat (60 m), Advanced Space borne Thermal Emission and
96 Reflection Radiometer (ASTER) (90 m), and MODIS (1020 m) independently to estimate ET over the Walnut Creek
97 watershed in Iowa. They compared these remote sensing estimates to eddy covariance flux measurements and
98 reported that Landsat and ASTER ET estimates had a higher degree of consistency with one another and correlated
99 better to the ground measurements ($r=0.87$ and $r=0.81$, respectively) than MODIS- based ET estimates did. All three
100 remote sensing products overestimated ET as compared to ground measurements (at 12 out of 14 tower sites).
101 Upon aggregation of Landsat and ASTER retrievals to MODIS scale (1 km), the correlation with the ground
102 measurements decreased to $r=0.75$ and $r=0.63$ for Landsat and ASTER, respectively.

103
104 Contrary to overestimation bias, many remotely sensed ET estimates that include parameters related to
105 aerodynamic resistance are significantly affected by heterogeneity, and underestimate ET as the scale increases
106 (Ershadi et al., 2013). Because aerodynamic resistance is significantly affected by land surface properties (e.g.,
107 vegetation height, roughness length, and displacement height), decreases in aerodynamic resistance at coarser
108 resolutions could lead to smaller estimates of evapotranspiration. Ershadi et al. (2013) showed that input
109 aggregation from 120m to 960 m in Surface Energy Balance System (SEBS, Su, 2002) leads to up to 15 %
110 underestimation of ET at the larger grid resolution in a study area in the south-east of Australia.

111

112 Rouholahnejad Freund and Kirchner (2017) quantified the impact of sub-grid heterogeneity on grid-average ET
113 using a simple Budyko curve (Turc, 1954; Mezentsev, 1955) in which long-term average ET is a non-linear function
114 of long-term averages of precipitation (P) and potential evaporation (PET). They showed mathematically that
115 averaging over spatially heterogeneous P and PET results in overestimation of ET within the Budyko framework (Fig.
116 1). Their analysis implies that large-scale ESMs that overlook land surface heterogeneity will also yield biased
117 evapotranspiration estimates due to the inherent nonlinearity in ET processes. They did not, however, determine
118 where around the globe, and under what conditions, this heterogeneity bias is likely to be most important.
119

120 The recognition that spatial averaging can potentially lead to biased flux estimates has prompted methods for
121 representing sub-grid-scale heterogeneities and processes within large scale land surface models and ESMs.
122 Accounting for land surface heterogeneity in large-scale ESMs is not merely constrained by limitations in both
123 computational power (Baker et al. 2017) and the availability of high-resolution forcing data, but also by the fact
124 that the atmospheric and land surface components of some ESMs operate at different resolutions. There have been
125 several attempts to integrate sub-grid heterogeneity in ESMs while keeping the computational costs affordable. In
126 “mosaic” approaches, the model is run separately for each surface type in a grid cell, and then the surface-specific
127 fluxes are area-weighted to calculate the grid-cell average fluxes (e.g., Avissar and Pielke, 1989; Koster and Suarez,
128 1992). The “effective parameter” approach (e.g., Wood and Mason, 1991; Mahrt et al., 1992), by contrast, seeks to
129 estimate effective parameter values at the grid cell scale that subsume the effects of sub-grid heterogeneity.
130 Estimating these effective parameters can be challenging because the relevant land-surface processes typically
131 depend nonlinearly on multiple interacting parameters, and land-surface signals at different scales are propagated
132 and diffused differently in the atmosphere. Alternatively, the “correction factor” approach (e.g., Maayar and Chen,
133 2006) uses sub-grid information on spatially heterogeneous land-surface processes and properties to estimate
134 multiplicative correction factors for fluxes that are originally calculated from spatially averaged inputs at the grid-
135 cell scale. All three approaches try to reduce the heterogeneous problem to a homogeneous one that has
136 equivalent effects on the atmosphere at the grid-cell scale.
137

138 There is a growing need to understand how sub-grid heterogeneity (and the atmosphere’s integration of it) affect
139 grid-scale water and energy fluxes, and to develop effective methods to incorporate these effects in ESMs (Clark et
140 al., 2015, Fan et al., 2019). In a previous study, we proposed a general framework for quantifying systematic biases
141 in ET estimates due to averaging over heterogeneities (Rouholahnejad Freund and Kirchner, 2017). We used the
142 Budyko framework as a simple estimator of ET, and demonstrated theoretically how averaging over heterogeneous
143 precipitation and potential evapotranspiration can lead to systematic overestimation of long-term average ET
144 fluxes from heterogeneous landscapes. In the present study, we apply this analysis across the globe and highlight
145 the locations where the [resulting](#) heterogeneity bias is largest. Our hypotheses, derived from the Budyko
146 framework as summarized in Eq. (4) below, are that (1) strongly heterogeneous landscapes, such as mountainous

147 terrain, will exhibit greater heterogeneity bias, (2) this bias will be larger in climates where P and PET are inversely
148 correlated in space, and (3) heterogeneity bias will decrease as the spatial scales of averaging decrease.

149

150 2. Effects of sub-grid heterogeneity on ET estimates in the Budyko framework

151 Budyko (1974) showed that long-term annual average evapotranspiration is a function of both the supply of water
152 (precipitation, P) and the evaporative demand (potential evapotranspiration, PET) under steady-state conditions
153 and in catchments with negligible changes in storage (Eq. 1; Turc, 1954; Mezentsev, 1955):

$$154 \quad ET = f(P, PET) = \frac{P}{\left(\left(\frac{P}{PET}\right)^n + 1\right)^{1/n}} \quad (1)$$

155 where ET is actual evapotranspiration, P is precipitation, PET is potential evaporation, and n (dimensionless) is a
156 catchment-specific parameter that modifies the partitioning of P between ET and discharge.

157

158 Evapotranspiration rates are inherently bounded by energy and water limits. Under arid conditions ET is limited by
159 the available supply of water (the water limit line in Fig. 1b), while under humid conditions ET is limited by
160 atmospheric demand (PET) and converges toward PET (the energy limit line in Fig. 1b). Budyko showed that over a
161 long period and under steady-state conditions, hydrological systems function close to their energy or water limits.
162 These intrinsic water and energy constraints make the Budyko curve downward-curving.

163

164 In a heterogeneous landscape, like the simple example of two model columns in Fig. 1a, P and PET vary spatially.
165 The two columns with heterogeneous P and PET are represented by the two solid black circles on the Budyko curve
166 in Fig. 1b. In this hypothetical two-column example, the true average of ET values calculated from individual
167 heterogeneous inputs (the solid black circles) lies below the curve (the grey circle, labeled "true average").
168 However, if we aggregate the two columns and consider the system as one column with average properties, the
169 function of average inputs (averaged P and PET over the two columns) lies on the Budyko curve (the open circle)
170 which is larger than the true average of the two columns. In short, in any downward curving function, the function
171 of the average inputs (the open circle) will always be larger than the average of the individual function values (the
172 true average; grey circle). The difference between the two can be termed the "heterogeneity bias".

173

174 In a previous study (Rouholahnejad Freund and Kirchner, 2017) we showed that when nonlinear underlying
175 relationships are used to predict average behaviour from averaged properties, the magnitude of the resulting
176 heterogeneity bias can be estimated from the degree of the curvature in the underlying function and the range
177 spanned by the individual data being averaged. Here we summarize these findings as building blocks of the current
178 study. The second-order, second-moment Taylor expansion of the ET function $f(P, PET)$ (Eq. 1) around its mean
179 directly yields:

Formatted: Font: Italic, Complex Script Font: Italic

180
$$\bar{f}(P, PET) = \overline{ET} \approx f(\bar{P}, \overline{PET}) + \frac{1}{2} \frac{\partial^2 f}{\partial P^2} \text{var}(P) + \frac{1}{2} \frac{\partial^2 f}{\partial PET^2} \text{var}(PET) + \frac{\partial^2 f}{\partial P \partial PET} \text{cov}(P, PET) \quad , \quad (2)$$

181 where $\bar{f}(P, PET)$ is the true average of the spatially heterogeneous ET function, $f(\bar{P}, \overline{PET})$ is the ET function
 182 evaluated at its average inputs \bar{P} and \overline{PET} , and the derivatives are calculated at \bar{P} and \overline{PET} . Evaluating the
 183 derivatives using Eq. (1) and reshuffling the terms, Rouholahnejad Freund and Kirchner (2017) obtained the
 184 following expression for the heterogeneity bias, the difference between the average ET, $\bar{f}(P, PET)$, and the ET
 185 function evaluated at the mean of its inputs, $f(\bar{P}, \overline{PET})$:

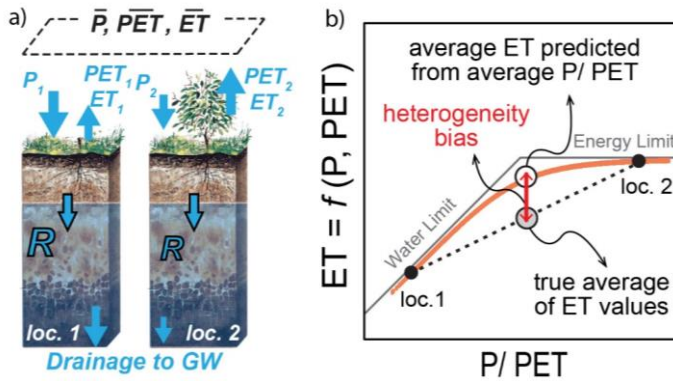
186
$$f(\bar{P}, \overline{PET}) - \bar{f}(P, PET) \approx (n+1) \frac{\bar{P}^{n+1} \overline{PET}^{n+1}}{(\bar{P}^n + \overline{PET}^n)^{2+1/n}} \left[\frac{1}{2} \frac{\text{var}(P)}{\bar{P}^2} + \frac{1}{2} \frac{\text{var}(PET)}{\overline{PET}^2} - \frac{\text{cov}(P, PET)}{\bar{P} \overline{PET}} \right]. \quad (3)$$

187 To more clearly show the effects of variations in P and PET, Eq. (3) can be reformulated as follows:

188
$$(n+1) \frac{\bar{P}^{n+1} \overline{PET}^{n+1}}{(\bar{P}^n + \overline{PET}^n)^{2+1/n}} \left[\frac{1}{2} \left(\frac{SD(P)}{\bar{P}} \right)^2 + \frac{1}{2} \left(\frac{SD(PET)}{\overline{PET}} \right)^2 - r_{P,PET} \left(\frac{SD(P)}{\bar{P}} \right) \left(\frac{SD(PET)}{\overline{PET}} \right) \right]. \quad (4)$$

189 Equation (4) shows that the heterogeneity bias depends on only four quantities: the fractional variation (i.e., the
 190 coefficient of variation) in precipitation $\left(\frac{SD(P)}{\bar{P}} \right)$ and in potential ET $\left(\frac{SD(PET)}{\overline{PET}} \right)$, the correlation between precipitation
 191 and potential ET ($r_{P,PET}$), and the function $(n+1) \frac{\bar{P}^{n+1} \overline{PET}^{n+1}}{(\bar{P}^n + \overline{PET}^n)^{2+1/n}}$, which quantifies the curvature in the ET function
 192 in Budyko space. As shown by Fig. 1b and Eq. (2), the discrepancy between average of the ET function and the ET
 193 function of the average inputs (the heterogeneity bias) is proportional to both the degree of nonlinearity in the
 194 function, as defined by its second derivatives, and the variability of P and PET. Equation (4) allows one to estimate
 195 how much the curvature of the ET function and the fractional variability (standard deviation divided by mean) of P
 196 and PET will affect estimates of ET. However, to the best of our knowledge, the consequences of these
 197 nonlinearities for global evaporative flux estimates have not previously been quantified.

198



199

200 Figure 1. Heterogeneity bias in a hypothetical two-column model in the Budyko framework. The true average ET of
201 the columns (gray circle) lies below the curve and is less than the average ET estimated from the average P/PET of
202 the two columns (open circle). The heterogeneity bias depends on the curvature of the function and the spread of
203 its inputs. Both panels are adapted from Rouholahnejad Freund and Kirchner (2017).

204

205 3. Effects of sub-grid heterogeneity on ET estimates at 1° by 1° grid scale across the globe

206 Across a landscape of similar size to a typical ESM grid cell (1° by 1°), soil moisture, atmospheric demand (PET) and
207 precipitation (P) will vary with topographic position; hillslopes will typically be drier, and riparian regions will be
208 wetter. To map the spatial pattern in the heterogeneity bias that ~~results could result~~ from averaging over this land
209 surface heterogeneity, we applied the approach outlined in section 2 to the global land surface area at 1° by 1° grid
210 scale. Within each 1° by 1° grid cell, we used 30 arc-second values of P (WorldClim; Hijmans et al., 2005) and PET
211 (WorldClim; Hijmans et al., 2005) to examine the variations in small-scale climatic drivers of ET. Because 30 arc-
212 seconds is nearly 1 km, hereafter we refer to the 30 arc-second data as 1km values for simplicity. The spatial
213 distribution of long-term annual averages (1960-1990) of P and PET values at 1 km resolution, along with 1km
214 values of the aridity index (AI=P/PET), are shown in Fig 2a-c. ET values calculated from these 1km P and PET values
215 using Eq. (1) are then averaged at 1° by 1° scale (“true average”, Fig. 2e). We also averaged the 1km values of P and
216 PET within each grid cell and then modeled ET using the Budyko curve (Eq. 1) applied to these averaged input
217 values. The difference between these two ET estimates is the heterogeneity bias.

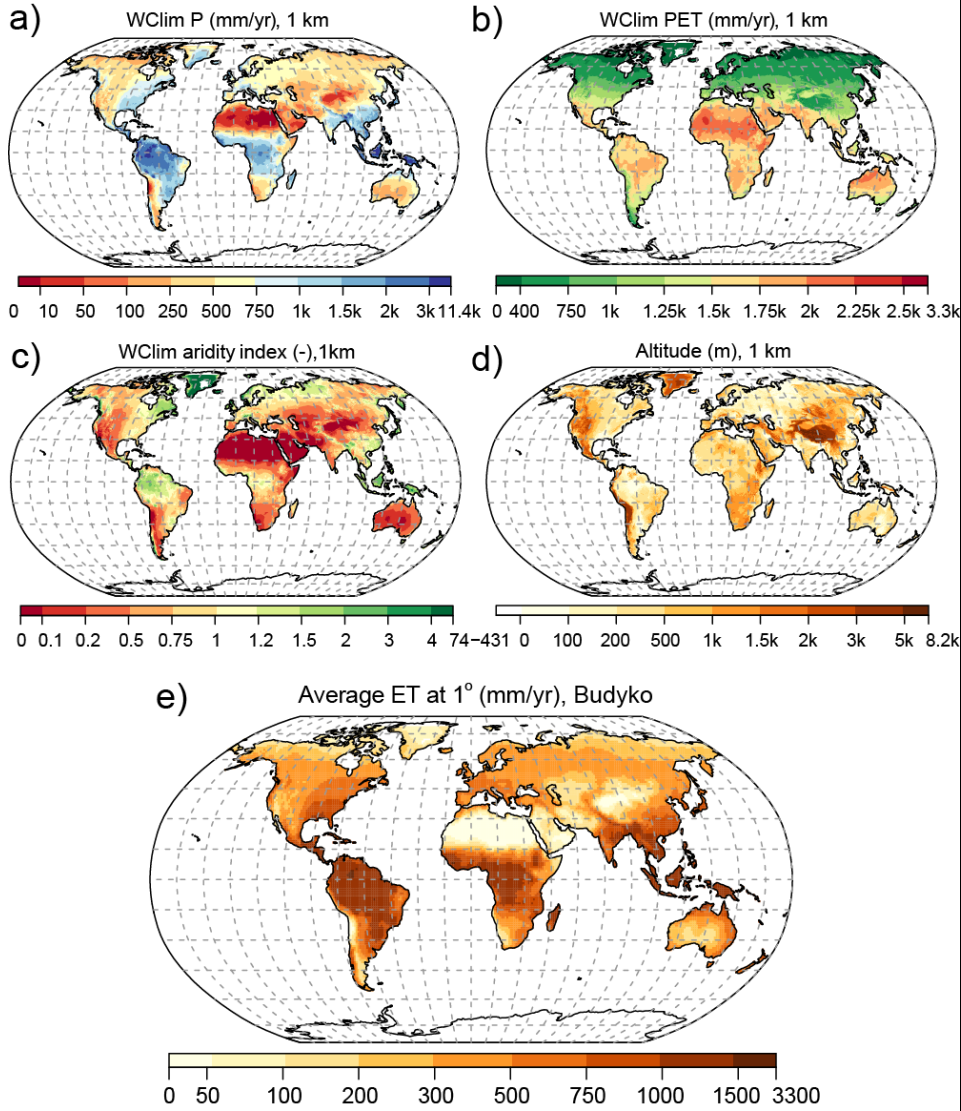
218

219 We also calculated the heterogeneity bias using Eq. (4), which describes how the nonlinearity in the governing
220 equation and the heterogeneity in P and PET jointly contribute to the heterogeneity bias. The heterogeneity bias
221 estimates obtained by Eq. (4) were functionally equivalent ($R^2=0.97$, root mean square error of 0.17%) to those
222 obtained by direct calculation using Eq. (1) as described above.

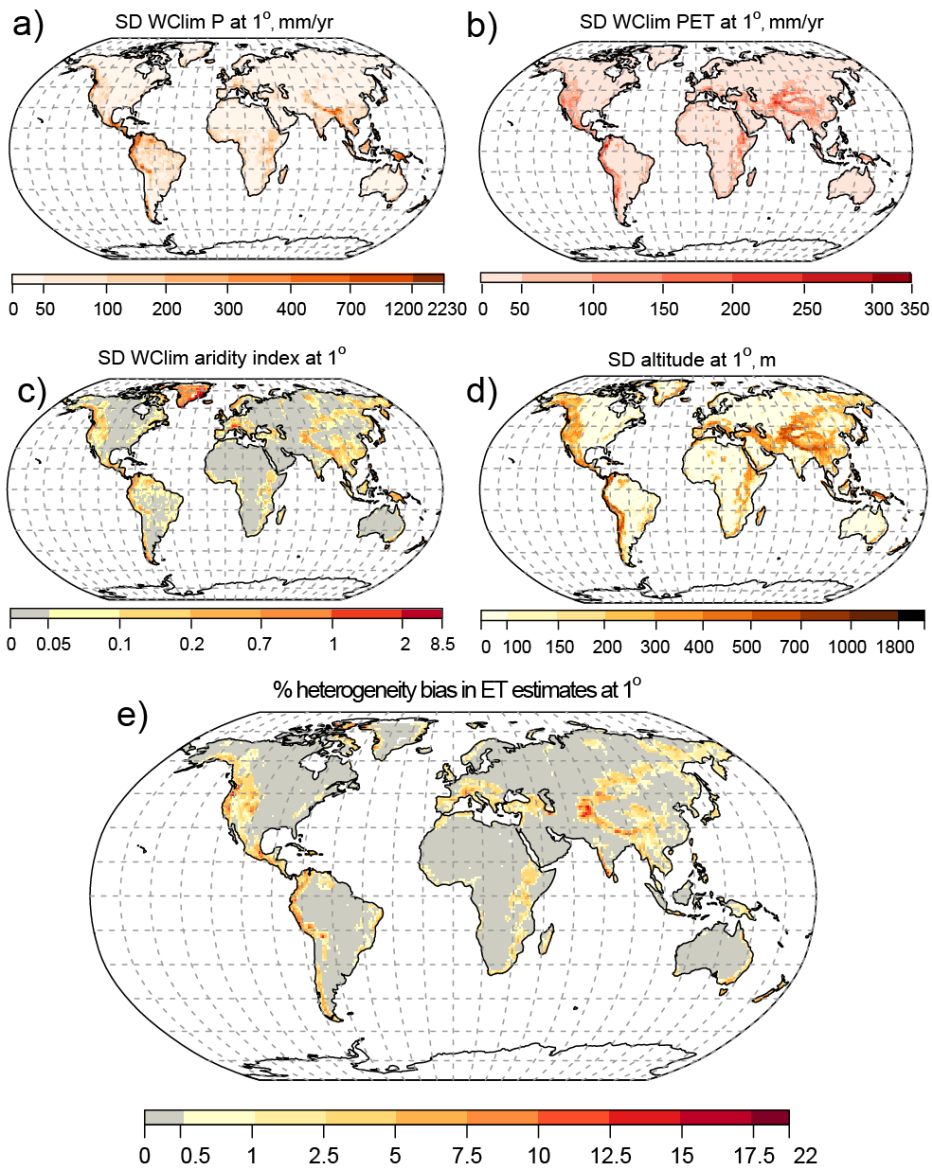
223

224 Fig. 3a-d illustrates the variability (quantified by standard deviation) of 1km values of P, PET, aridity index, and
225 altitude at the 1° by 1° grid scale. The heterogeneity bias in long-term average ET fluxes at the 1° by 1° grid scale
226 (Fig. 3e) highlights regions around the globe where ET fluxes are likely to be systematically overestimated. The
227 spatial distribution of the heterogeneity bias calculated using Eq. 4 (Fig. 3e) closely coincides with locations where
228 the aridity index is highly variable (Fig. 3c), which is driven in turn by topographic variability (Fig. 3d). Strongly
229 heterogeneous landscapes exhibit ~~significant-larger estimated~~ heterogeneity biases in long-term average ET fluxes.
230 Although the global average ~~of our Budyko-based~~ heterogeneity bias ~~estimates~~ is small (<1%), physically based ET
231 calculations may exhibit larger heterogeneity biases than the modest values we calculate here, because the Budyko
232 approach already subsumes spatial heterogeneity effects at the catchment scale (and also temporal heterogeneity
233 effects due to its steady-state assumptions). The heterogeneity biases in ET estimates shown in Fig. 3e correspond
234 to long-term average ET estimates. Given the fact that P and PET can vary temporally (i.e., seasonality), the actual
235 bias could be much larger, particularly where P and PET are inversely correlated (see the last term of Eq. 4).

236
237 Our results show that the topographic gradient, and hence the variability in the aridity index across a given grid
238 scale, drives consistent, predictable patterns of heterogeneity bias in evapotranspiration estimates at that scale.
239 Equation 4 shows that this bias is equally sensitive to fractional variability in P and PET (standard deviation divided
240 by mean). However, because P is typically more variable (in percentage terms) than PET across landscapes, the
241 variability in P will usually make a larger contribution to the estimated heterogeneity bias.



243
 244 Figure 2. Global distribution of one-kilometer resolution annual mean precipitation (a: P; WorldClim; Hijmans et al.,
 245 2005), potential evapotranspiration (b: PET; WorldClim; Hijmans et al., 2005), aridity index (c: AI=P/PET; WorldClim;
 246 Hijmans et al., 2005), and topography (d: SRTM; Jarvis et al., 2008), along with (e) evapotranspiration (ET) at 1° by
 247 1° scale by averaging 1km values of ET calculated using the Budyko function (Eq. 1).
 248



249
 250 Figure 3. Global spatial distribution of variability (standard deviation) of one-kilometer values of a) precipitation (P),
 251 b) potential evapotranspiration (PET), c) aridity index (AI=P/PET), and d) altitude at 1° by 1° grid cell. The
 252 heterogeneity bias in ET estimates (e) is calculated using Eq. (4). Grid cells with larger standard deviation in altitude
 253 and aridity index have larger heterogeneity bias.

254 **4. Variation in heterogeneity bias across climate zones, data sources, and grid scales**

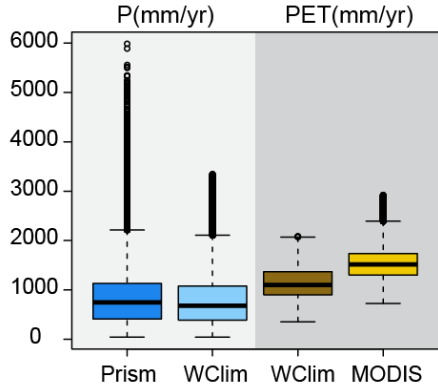
255 With increased availability of spatial data, it is becoming standard practice to assess input data uncertainties and
256 their propagated impacts on water and energy flux estimates in land surface models. To quantify how choices
257 among alternative input data products could affect the heterogeneity bias in ET estimates, we calculated the
258 heterogeneity bias at 1° by 1° grid cell resolution across the contiguous US using four different pairs of P and PET
259 data products. Two precipitation data sets, Prism (<http://prism.oregonstate.edu>) and WorldClim (Hijmans et al.,
260 2005), along with two PET data sets, MODIS (Mu et al., 2007) and WorldClim (Hijmans et al., 2005). As Prism
261 precipitation data is available at 4 km resolution, all other data sets were aggregated to 4 km. Two P products and
262 two PET products were combined in all possible pairs. The WorldClim PET dataset (Hijmans et al., 2005) is based on
263 the Hargreaves method (Hargreaves and Samani 1985) while the MODIS PET product (Mu et al, 2007) is based on
264 the Penman–Monteith equation (Monteith, 1965). The heterogeneity bias in ET estimates (Eq. 4), as outlined in
265 Sect. 2, was evaluated from 4km values of P, PET, and the estimated average ET using the Budyko relationship (Eq.
266 1) for each of the four input data pairs. Figure 4a-e compares the spatial distributions of heterogeneity bias across
267 the contiguous US for the four pairs of P and PET data products. The heterogeneity bias in ET estimates reached as
268 high as 36 % in the western US using Prism P and WorldClim PET as input to the ET model (Fig. 4b). A visual
269 comparison of Figs. 4b and Fig. 4d shows that the choice of P data source (Prism vs. WorldClim) had a bigger effect
270 on the heterogeneity bias than the choice of PET data source (MODIS vs. WorldClim), meaning that the fractional
271 variability in P is the dominant variable. In all cases, data sources that were more variable in relation to their means
272 (Prism for P and WorldClim for PET; Fig. 4b) led to larger estimates of heterogeneity biases, as expected from Eq.
273 (4). Thus we infer that we would have obtained larger heterogeneity biases if we had conducted our global analysis
274 (Fig. 3) with Prism P and either WorldClim or MODIS PET, but we cannot show that result explicitly at global scale
275 because Prism P is not freely available globally.

276
277 If we separate the heterogeneity biases shown in Fig. 4 according to Köppen-Geiger climate zones (Peel et al., 2007;
278 Fig. 5a), we see that they are distinctly higher in particular climate-terrain combinations. Estimated hHeterogeneity
279 biases are higher in regions with temperate climates and dry summers (climate zone Cs) and in regions with cold,
280 dry summers (climate zone Ds), most likely due to the sharp spatial gradient in their water and energy sources for
281 evapotranspiration (Fig. 5b). These areas typically have high topographic relief, combined with seasonal climate.
282 The heterogeneity effects on ET estimates in these regions are expected to be even larger when a mechanistic
283 model of ET is used. We expect that averaging over temporal variations of drivers of ET, especially in places with
284 strong seasonality, could substantially bias the ET estimates, but this cannot be quantified in the Budyko framework
285 due to its underlying steady-state assumptions. Figure 5b also illustrates the relative magnitudes of the
286 heterogeneity biases obtained with the four pairs of P and PET data sources. The estimated heterogeneity bias is
287 ~~the~~ highest when the Prism P and WorldClim PET datasets are used, followed by the combination of Prism P and
288 MODIS PET, which resulted in the second-highest heterogeneity bias across different climate zones. Wilcoxon
289 signed-rank tests was performed to evaluate the statistical significance of the differences between heterogeneity

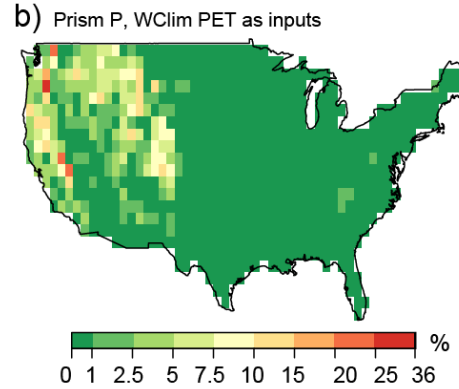
290 bias in ET estimates using all pairs of climate zones and data sources that are shown in Fig. 5b (Table S1). These
291 analysis show that while the difference between heterogeneity biases estimated in Cs and Ds climate zones are not
292 statistically significant across all four combinations of datasets, the difference between estimated heterogeneity
293 bias in Cs versus Cf, Ds versus Cf, as well as Cs versus Bs climate zones are significant across all four data
294 combinations (highlighted in Table S1 of the supplementary material).

295
296 Equation 4 shows that heterogeneity biases in Budyko estimates of ET are equally sensitive to the same percentage
297 variability in P and PET. Thus the degree of sensitivity, per se, to P and PET variations expressed in percentage terms
298 is the same. Although Figs. 5c and 5d give the visual impression that PET is more variable than P across climate
299 zones and between data sources, Fig. 5e shows that the fractional variability in P is systematically higher than PET,
300 and it also varies more across the climate zones and between the two data sets. Because P is typically more
301 variable than PET (in percentage terms) across landscapes, the variability in P will make a larger contribution to the
302 heterogeneity bias (Fig. 5e) ~~estimated using~~ the Budyko approach. Whether this is true for more physically based
303 ET estimates remains to be seen. Analysis of percent variability of P and PET products shows that percent
304 variabilities of precipitation products are in general larger than PET products and hence contribute more to
305 heterogeneity (Fig 5e). While the percent variabilities of the two PET products are in the same range, the percent
306 variability in Prism precipitation is slightly larger than in WorldClim precipitation, in regions with dry summers (Cs
307 and Ds climate zones in Fig. 5a).
308

a) Distribution of P and PET in the four datasets

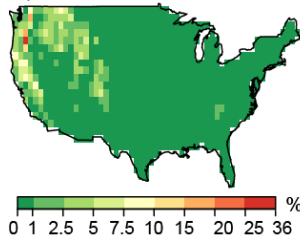


% heterogeneity bias in ET estimates at 1°

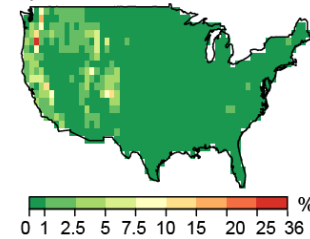


% heterogeneity bias in ET estimates at 1°

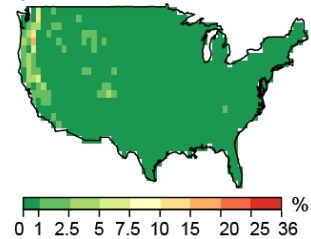
c) Prism P, MODIS PET as inputs



d) WorldClim P, WorldClim PET as inputs

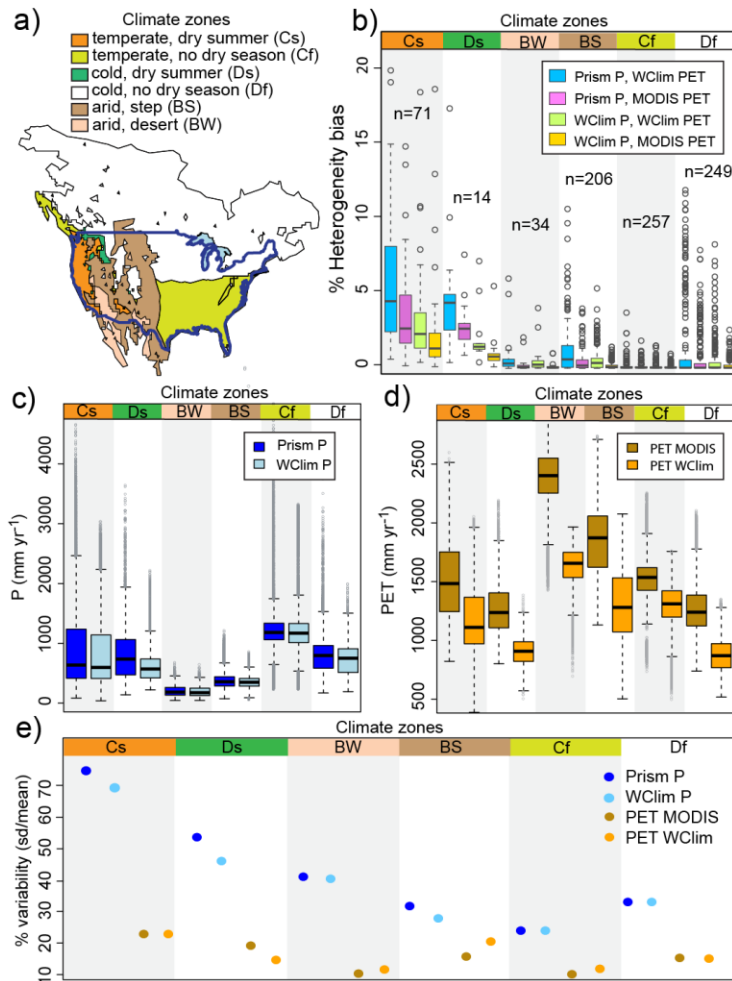


e) WorldClim P, MODIS PET as inputs



309

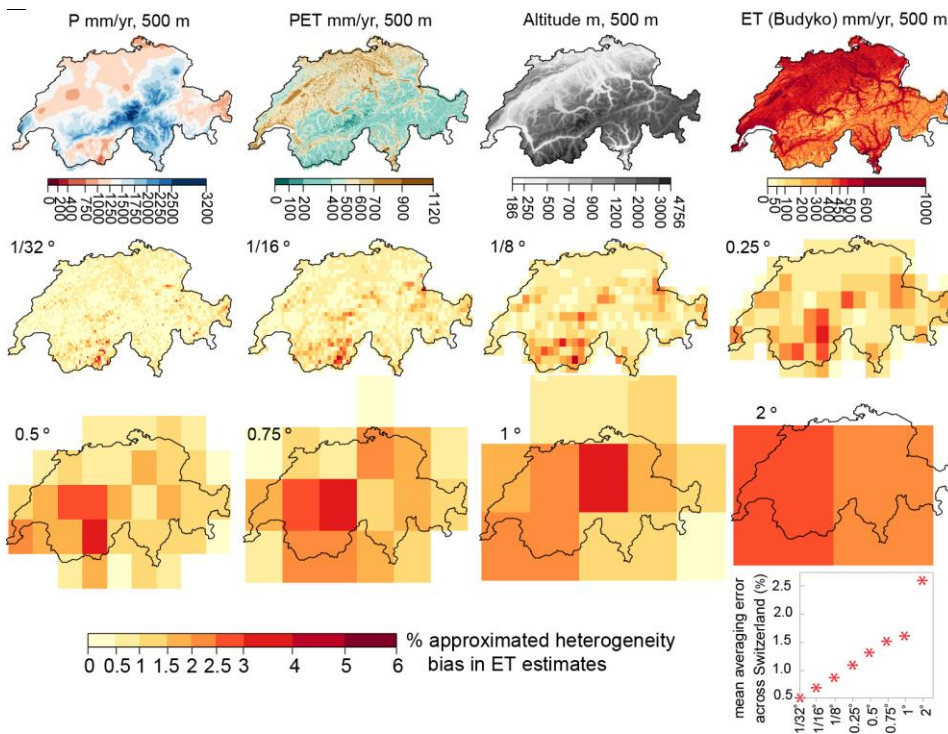
310 Figure 4. The distribution of P and PET in the four datasets is shown in a). Estimated heterogeneity bias (Eq. 4)
 311 across the contiguous US using four-kilometer values of b) Prism P and WorldClim PET c) Prism P and MODIS PET d)
 312 WorldClim P and WorldClim PET, and e) WorldClim P and MODIS PET as inputs.
 313



314
 315 Figure 5. a) Köppen-Geiger climate classification (Peel et al., 2007 in Beck et al. 2013) across the contiguous US, b)
 316 the distribution of calculated heterogeneity bias in ET estimates (Eq. 4) at 1° by 1° grid cell in individual climate
 317 zones, shown by boxplot (three data points with heterogeneity biases of over 20% are off-scale). The significance of
 318 differences between the pairs are presented in Table S1. Panels c and d show the distribution of precipitation
 319 products (Prism and WorldClim) and potential evaporation products (MODIS and WorldClim) at individual climate
 320 zones, respectively. The color-coded climate zones at the tops of panels b, c, and d correspond to the climate zones
 321 mapped in panel a. Panel e compares the percentage variability of the two P and PET data products across climate
 322 zones, showing that the percentage variability in P is markedly higher than in PET, and the percentage variability in
 323 Prism P is somewhat higher than in WorldClim P, particularly in climate zones with dry summers.

324 Because future increases in computing power will lead to ESMs with smaller grid cells, it is useful to ask how
 325 changes in grid resolution affect the heterogeneity biases that we have estimated in this paper. To quantify the
 326 heterogeneity bias in ET estimates as a function of grid scale, we repeated our analysis at various grid resolutions
 327 using Switzerland as a test case. We started with high-resolution (500m) maps of long-term average annual
 328 precipitation and PET across the Swiss landscape (Fig. 6), and then used Eq. 4 to estimate the heterogeneity bias at
 329 grid scales ranging from 1/32° to 2° (~3 km to ~200 km). As Fig. 6 shows, aggregating P and PET over larger scales
 330 leads to larger, and more widespread, overestimates in ET. Conversely, at finer grid resolutions, the average
 331 heterogeneity bias is smaller, and the locations with large biases are more localized. On average, the heterogeneity
 332 bias across Switzerland as a whole grows exponentially as the inputs are averaged over larger grids (as shown in the
 333 lower-right panel in Fig. 6).

334
 335



336

337 Figure 6. Heterogeneity bias in ET estimates at various scales across Switzerland, estimated from 500m climate
 338 data. ET is calculated using the Budyko relationship (Eq. 1). Heterogeneity bias was estimated from 500m
 339 precipitation (P) and potential evapotranspiration (PET), and their variances at each grid scale, using Eq. 4. At finer
 340 grid resolutions, the heterogeneity bias is more localized, and smaller on average.

341

342 **5. Summary and discussion**

343 Because evapotranspiration (ET) processes are inherently bounded by water and energy constraints, over the long
344 term, ET is always a nonlinear function of available water and PET, whether this function is expressed as a Budyko
345 curve or another ET model. These nonlinearities imply that spatial heterogeneity will not simply average out in
346 predictions of land surface water and energy fluxes ~~in ESMs~~. Overlooking sub-grid spatial heterogeneity in large-
347 scale ~~land surface models ESMs~~ could lead to biases in ~~estimating estimated water and energy fluxes~~ these fluxes
348 ~~(e.g., ET rates)~~. Here we have shown that, across several scales, averaging over spatially heterogeneous land
349 surface properties and processes leads to biases in evapotranspiration estimates. We examined the global
350 distribution of this bias, its scale dependence, and its sensitivity to variations in P versus PET, and showed under
351 what conditions, ~~this heterogeneity bias is likely to be most important~~. Our analysis does not quantify the
352 heterogeneity biases in ESMs, owing to the many differences between these mechanistic models and the simple
353 empirical Budyko curve. But if the heterogeneity biases in ESMs can be quantified, they can be used as correction
354 factors to improve ESM estimates of surface-atmosphere water and energy fluxes across landscapes. Our paper
355 highlights a general methodology that can be used to estimate heterogeneity biases and to map their spatial
356 patterns, but not to calculate their absolute magnitudes because those will change significantly depending on the
357 ET formulation that is used.

358
359 In this study, we used Budyko curves as simple models of ET, in which long-term average ET rates are functionally
360 related to long-term averages of P and PET. We used an approach outlined by Rouholahnejad Freund and Kirchner
361 (2017) to estimate the heterogeneity bias in modeled ET at 1-degree grid scale across the globe (Fig. 3), and also at
362 multiple grid scales across Switzerland (Fig. 6), using finer-resolution P and PET values as drivers of ET. We showed
363 how the heterogeneity effects on ET estimates vary with the nonlinearity in the governing equations and with the
364 variability in land surface properties. Our analysis shows that heterogeneity effects on ET fluxes matter the most in
365 areas with sharp gradients in the aridity index, which are in turn controlled by topographic gradients, and not
366 merely in areas that are either arid or humid (e.g., compare Fig. 3e with Fig. 2c).

367
368 According to our analysis, regions within the U.S. that have temperate climates and dry summers exhibit greater
369 heterogeneity bias in ET estimates (Fig. 5). We show that the estimated heterogeneity bias ~~in ET estimates~~ at each
370 grid scale depends on the variance in the drivers of ET at that scale (Fig. 4), and on the choice of data sources used
371 to estimate ET. Heterogeneity bias ~~estimates were~~ was significantly larger across the contiguous United States
372 when P and PET data sources with larger variances were used (Fig. 4).

373
374 We also explored how heterogeneity biases and their spatial distribution vary with the magnitude and spatial
375 distribution of heterogeneity bias in ET estimates as a function of the scale at which the climatic drivers of ET are
376 averaged. We found that as heterogeneous climatic variables are aggregated to larger scales, the heterogeneity
377 biases in ET estimates become greater on average, and extend over larger areas (Fig. 6). At smaller grid scales,

378 ~~estimated the heterogeneity bias~~ heterogeneity biases do ~~does~~ not completely disappear, but instead becomes
379 more localized around areas with sharp topographic gradients. Finding an effective scale at which one can average
380 over the heterogeneity of land surface properties and processes has been a longstanding problem in Earth science.
381 Our analysis shows that at smaller resolutions the average heterogeneity bias as seen from the atmosphere
382 becomes smaller, but there is no characteristic scale at which it vanishes entirely (Fig. 6). The magnitude and spatial
383 distribution of this bias depend strongly on the scale of the averaging and degree of the nonlinearity in the
384 underlying processes. The heterogeneity bias concept is general and extendable to any convex or concave function
385 (Rouholahnejad Freund and Kirchner 2017), meaning that in any nonlinear process, averaging over spatial and
386 temporal heterogeneity can potentially lead to bias.

387
388 In the analysis presented here, we have assumed a value of 2 for the Budyko parameter n , which approximates the
389 variation of ET/PET with respect to P/PET in MODIS and WorldClim data across continental Europe (Mu et al. 2007;
390 Hijmans et al. 2005; Rouholahnejad Freund & Kirchner, 2017). Although there are suggestions in the literature that
391 n can vary with land use and other landscape properties (e.g., Teuling et al., 2019), here we have assumed that n is
392 spatially and temporally constant in order to focus on the effects of heterogeneity in P and PET. In the supplement
393 we present a sensitivity analysis with values of n ranging from 2 to 5 (Fig. S1). That analysis shows that, as expected
394 from Eqs. 3 and 4, higher values of n lead to larger heterogeneity biases, because higher values of n localize the
395 curvature of the Budyko function more strongly at the transition between the energy and water limits (Fig. 1b),
396 increasing the heterogeneity bias for P/PET values near this transition. Nonetheless, but the spatial pattern shown
397 in Fig. 3e remains largely unchanged over the full range of n values that we analyzed, and t—The Taylor
398 approximation in Eqs. 3 and 4 yields realistic estimates of the heterogeneity bias for all values of n that were tested
399 (Fig. S2). Thus while our numerical estimates of heterogeneity bias depend somewhat on the value of n , our
400 conclusions do not.

401
402 One should keep in mind that the true mechanistic equations that determine point-scale ET as a function of point-
403 scale water availability and PET (if such data were available) may be much more nonlinear than Budyko's empirical
404 curves, because these curves already average over significant spatial and temporal heterogeneity. Thus, we expect
405 that the real-world effects of sub-grid heterogeneity are probably larger than those we have estimated in Sects. 3
406 and 4 of this study. In addition, the 1km P and PET values that are used in our global analysis might be still too
407 coarse to represent small-scale heterogeneity that is important to evapotranspiration processes.

408
409 Budyko curves are empirical relationships that functionally relate evaporation processes to the supply of water and
410 energy under steady-state conditions in closed catchments with no changes in storage. Our analysis likewise
411 assumes no changes in storage, nor any lateral transfer between the model grid cells, although both lateral
412 transfers and changes in storage may be important, both in the real world and in models. Unlike the Budyko
413 framework, ET fluxes in most ESMs are often physically based (not merely functions of P and PET) and are

Formatted: Font: Italic, Complex Script Font: Italic

Formatted: Font: Italic, Complex Script Font: Italic

Formatted: Font: Italic, Complex Script Font: Italic

Formatted: Font: Italic, Complex Script Font: Italic

Formatted: Font: Italic, Complex Script Font: Italic

Formatted: Font: Italic, Complex Script Font: Italic

Formatted: Font: Italic, Complex Script Font: Italic

Formatted: Font: Italic, Complex Script Font: Italic

Formatted: Font: Italic, Complex Script Font: Italic

414 calculated at much smaller time steps (seconds to minutes). These models often represent more processes that are
415 important to evapotranspiration (such as storage variations) and include their dynamics to the extent that is
416 computationally feasible. Because these relationships may be much more nonlinear than Budyko curves, [much](#)
417 ~~larger there may also be significant~~ heterogeneity biases [could result](#) when complex physically based models are
418 used to estimate ET from spatially aggregated data. Therefore, we are now working to quantify heterogeneity bias
419 in ET fluxes using a more mechanistic land surface model.

420

421 **Acknowledgements**

422 E.R.F. acknowledges support from the Swiss National Science Foundation (SNSF) under Grant No. P2EZP2_162279.
423 The authors thank Massimiliano Zappa of the Swiss Federal Research Institute WSL for providing the 500m
424 resolution data that enabled the analysis shown in Fig. 6.

425

426 **References**

- 427 Aminzadeh M., and D. Or: The complementary relationship between actual and potential evaporation for spatially
428 heterogeneous surfaces, *Water Resour. Res.*, 53, 580–601, doi:10.1002/2016WR019759, 2017.
- 429 Avissar, R., R. A. Pielke: A Parameterization of Heterogeneous Land Surfaces for Atmospheric Numerical Models and
430 Its Impact on Regional Meteorology, *Monthly Weather Review*, vol. 117, issue 10, p. 2113, doi:10.1175/1520-
431 0493(1989)117<2113:APOHLS>2.0.CO;2, 1989.
- 432 Baker I. T. , P. J. Sellers , A. S. Denning, I. Medina , P. Kraus, K. D. Haynes , and S. C. Biraud: Closing the scale gap
433 between land surface parameterizations and GCMs with a new scheme, SiB3-Bins, *Journal of Advances in Modeling
434 Earth Systems*, *J. Adv. Model. Earth Syst.*, 9, 691–711, doi:10.1002/2016MS000764, 2017.
- 435 Bastiaanssen, W. G. M., M. Menenti, R. A. Feddes, and A. A. M. Holtslag: A remote sensing surface energy balance
436 algorithm for land (SEBAL): 1. Formulation, *Journal of Hydrology*, 212-213, 198–212, 1998.
- 437 Beck H. E., A. I. J. M. van Dijk, D. G. Miralles, R. A. M. de Jeu, L. A. Bruijnzeel, T. R. McVicar, and J. Schellekens:
438 Global patterns in base flow index and recession based on streamflow observations from 3394 catchments, *Water
439 Resour. Res.*, 49, 7843–7863, doi:10.1002/2013WR013918, 2013.
- 440 Boone, A., and O. J. Wetzel: A simple scheme for modeling sub-grid soil texture variability for use in an atmospheric
441 climate model. *Journal of the Meteorological Society of Japan*, 77(1), 317–333, 1998.
- 442 Budyko, M. I.: *Climate and life*, Academic, New York, 1974.
- 443 Clark, M. P., Y. Fan, D. M. Lawrence, J. C. Adam, D. Bolster, D. J. Gochis, R. P. Hooper, M. Kumar, L. R. Leung, D. S.
444 Mackay, R. M. Maxwell, C. Shen, S. C. Swenson, and X. Zeng: Improving the representation of hydrologic processes
445 in Earth System Models, *Water Resour. Res.*, 51, 5929–5956, doi:10.1002/2015WR017096, 2015.

446 Ershadi A., M. F. McCabe, J. P. Evans, J. P. Walker: Effects of spatial aggregation on the multi-scale estimation of
447 evapotranspiration, *Remote Sensing of Environment* 131, 51–62, <http://dx.doi.org/10.1016/j.rse.2012.12.007>,
448 2013.

449 Fan, Y., M. Clark, D. M. Lawrence, S. Swenson, L. E. Band, S. L. Brantley, P. D. Brooks, W. E. Dietrich, A. Flores, G.
450 Grant, J. W. Kirchner, D. S. Mackay, J. J. McDonnell, P. C. D. Milly, P. L. Sullivan, C. Tague, H. Ajami, N. Chaney, A.
451 Hartmann, P. Hazenberg, J. McNamara, J. Pelletier, J. Perket, E. Rouholahnejad-Freund, T. Wagener, X. Zeng, E.
452 Beighley, J. Buzan, M. Huang, B. Livneh, B. P. Mohanty, B. Nijssen, M. Safeeq, C. Shen, W. van Verseveld, J. Volk, D.
453 Yamazaki: Hillslope hydrology in global change research and Earth system modeling, *Water Resources Research*, 55,
454 doi:10.1029/2018WR023903, 2019.

455 [Giorgi, F., and R. Avissar: Representation of heterogeneity effects in Earth system modeling: Experience from land](#)
456 [surface modeling, *Rev. Geophys.*, 35, 413–437, doi:10.1029/97RG01754, 1997.](#)

457 Hargreaves, G. H., and Z. A. Samani: Reference crop evaporation from temperature, *Appl. Eng. Agric.*, 1(2), 96-99,
458 1985.

459 Hijmans, R. J., S. E. Cameron, J. L. Parra, P. G. Jones, and A. Jarvis: Very high resolution interpolated climate surfaces
460 for global land areas, *Int. J. Climatol.*, 25, 1965–1978, doi:10.1002/joc.1276, 2005.

461 Holland, S., J. L. Heitman, A. Howard, T. J. Sauer, W. Giese, A. Ben-Gal, N. Agam, D. Kool, and J. Havlin: Micro Bowen
462 ratio system for measuring evapotranspiration in a vineyard interrow, *Agric. For. Meteorol.*, 177, 93–100, 2013.

463 Hong, S. H., J. M. H. Hendrickx, and B. Borchers: Up-scaling of SEBAL derived evapotranspiration maps from Landsat
464 (30 m) to MODIS (250 m) scale, *Journal of Hydrology*, 370, 122–138, 2009.

465 Jarvis, A., Reuter, H. I., Nelson, A., and Guevara, E.: Hole-filled SRTM for the globe Version 4, available from the
466 CGIARCSI SRTM 90m Database, <http://srtm.csi.cgiar.org> (last access: 26 February 2016), 2008.

467 Kalma, J. D., T. R. McVicar, and M. F. McCabe: Estimating land surface evaporation: A review of methods using
468 remotely sensed surface temperature data, *Surv. Geophys.*, 29, 421–469, doi:10.1007/s10712-008-9037-z, 2008.

469 Kollet S. J.: Influence of soil heterogeneity on evapotranspiration under shallow water table conditions: transient,
470 stochastic simulations, *Environmental Research Letters*, 4, 35007, doi:10.1088/1748-9326/4/3/035007, 2009.

471 Koster R. D. et al.: GLACE: The Global Land– Atmosphere Coupling Experiment. Part I: Overview. *J. Hydrometeorol.*, 7,
472 590–610, 2006.

473 Koster R. D., and M. Suarez: Modeling the land surface boundary in climate models as a composite of independent
474 vegetation stands, *J. Geophysical Research*, 97 (D3), 26-97-2715, 1992.

475 [Lu, H., T., Liu, Y. Yang, D. Yao: A hybrid dual-Source model of estimating evapotranspiration over different](#)
476 [ecosystems and implications for satellite-based approaches, *Remote Sens.* 6, 8359–8386, 2014.](#)

477 Maayar, M. E., J. M. Chen: Spatial scaling of evapotranspiration as affected by heterogeneities in vegetation,
478 topography, and soil texture, *Remote Sensing of Environment*, 102, 33–51, 2006.

479 Mahrt, L., J. Sun, D. Vickers, J. I. MacPherson, J. R. Perderson, and R. L. Desjardins: Observations of fluxes and inland
480 breezes over a heterogeneous surface, *J. Atmos. Sci.* 51, 2165e2178, 1992.

481 McCabe M., and E. Wood: Scale influences on the remote estimation of evapotranspiration using multiple satellite
482 sensors, *Remote Sensing of Environment* 105 (2006) 271–285, 2006.

483 Mezentsev, V. S.: More on the calculation of average total evaporation, *Meteorol. Gidrol.*, 5, 24–26, 1955.

484 Montheith, J. L.: Evaporation and environment, the state of and movement of water in living organisms, *Proceeding*
485 *of Soc. for Exp. Biol.*, 19, 205-234, doi:10.1002/qj.49710745102, 1965.

486 Mu, Q., F. A. Heinsch, M. Zhao, and S. W. Running: Development of a global evapotranspiration algorithm based on
487 MODIS and global meteorology data, *Remote Sens. Environ.*, 111, 519–536, doi:10.1016/j.rse.2007.04.015, 2007.

488 Peel, M. C., B. L. Finlayson, and T. A. McMahon: Updated world map of the Köppen-Geiger climate classification,
489 *Hydrol. Earth Syst. Sci.*, 11, 1633-1644, <https://doi.org/10.5194/hess-11-1633-2007>, 2007.

490 PRISM Climate Group, Oregon State University, <http://prism.oregonstate.edu>, created 22 Feb 2017.

491 Rouholahnejad Freund, E., and J. W. Kirchner: A Budyko framework for estimating how spatial heterogeneity and
492 lateral moisture redistribution affect average evapotranspiration rates as seen from the atmosphere, *Hydrology*
493 *and Earth System Sciences*, 21(1), 217-233, 2017.

494 Santanello J. R., and C. D. Peters-Lidard: Diagnosing the Sensitivity of Local Land–Atmosphere Coupling via the Soil
495 Moisture–Boundary Layer Interaction, *J. Hydrometeorology*, 12, 766-786, doi: 10.1175/JHM-D-10-05014.1, 2011.

496 Sato N., P. J. Sellers, D. A. Randall, E. K. Schneider, J. Shukla, J. L. Kinter III, Y. T. Hou, and E. Albertazzi: Effects of
497 Implementing the Simple Biosphere Model in a General Circulation Model, *J. Atmospheric Sciences*, 46(18), 2757-
498 2782, 1989.

499 Seneviratne, S. I., T. Corti, E. L. Davin, M. Hirschi, E. B. Jaeger, I. Lehner, B. Orlowsky, and A. J. Teuling: Investigating
500 soil moisture–climate interactions in a changing climate: A review, *Earth-Science Reviews*, 99(3–4), 125-161, 2010.

501 Shahraeeni, E., and D. Or: Thermo-evaporative fluxes from heterogeneous porous surfaces resolved by infrared
502 thermography, *Water Resour. Res.*, 46, W09511, doi:10.1029/2009WR008455, 2010.

503 Su, Z.: The Surface Energy Balance System (SEBS) for estimation of turbulent heat fluxes. *Hydrology and Earth*
504 *System Sciences*, 6, 85–100, 2002.

505 Teuling, A. J. and de Badts, E. A. G. and Jansen, F. A. and Fuchs, R. and Buitink, J. and Hoek van Dijke, A. J. and
506 Sterling, S. M., Climate change, reforestation/afforestation, and urbanization impacts on evapotranspiration and
507 streamflow in Europe, *Hydrology and Earth System Sciences*, 23, 3631–3652, DOI = {10.5194/hess-23-3631-2019,
508 2019}. Turc, L.: Le bilan d'eau des sols: relation entre la precipitations, l'évaporation et l'écoulement, *Ann. Agron. A*,
509 5, 491–569, 1954.

510 Wood, N., and P. J. Mason: The influence of static stability on the effective roughness length for momentum and
511 heat transfer, *Quart. J. Roy. Meteor. Soc.* 117, 1025e1056, 1991.